Bi-objective analytics of 3D visual-physical nature exposures in high-rise high-density cities for landscape and urban planning

Maosu Li[1], Fan Xue[2*], and Anthony G. O. Yeh[3]

Abstract

Urban dwellers enjoy nature exposure in the neighborhood built environment through visual and physical ways, such as window views and outdoor activities. However, existing studies and analytics examine these pathways separately, leading to underinformed urban planning practices such as difficult prioritizing urban areas with both low-level nature exposures. The underinformation problem is particularly severe for high-rise, high-density cities that embrace high-level vertical diversity. This study aims to propose bi-objective analytics of 3D visual-physical nature exposures, for holistic – rather than separated – assessments. First, a floor-level Nature Exposure Index (*NEI*) is defined with visual and physical components. The visual component NEI_v is assessed by window view imagery and deep transfer learning, while the physical component NEI_p reflects the mean time from the floor to the nearest natural sites (e.g., nature parks and seaside) through the 3D pedestrian network. Then, bi-objective optimization-based analytics is designed for (i) identifying buildings and blocks with holistically low-level visual-physical nature exposures using *NEI* and (ii) examining

[1] Maosu LI, PhD Candidate.
Department of Urban Planning and Design, The University of Hong Kong, Pokfulam, Hong Kong SAR, China; Email: maosulee@connect.hku.hk, : https://orcid.org/0000-0002-9970-4053

[2] Fan XUE, Assistant Professor.
Department of Real Estate and Construction, The University of Hong Kong, Pokfulam, Hong Kong SAR, China; Email: xuef@hku.hk, : http://orcid.org/0000-0003-2217-3693
*: Corresponding author, Tel: +852 3917 4174, Fax: +852 2559 9457; Email: xuef@hku.hk

[3] Anthony G. O. YEH, Chair Professor.
Department of Urban Planning and Design, The University of Hong Kong, Pokfulam, Hong Kong SAR, China; Email: hdxugoy@hku.hk, : http://orcid.org/0000-0002-0587-0588

probabilistic outputs and robustness of linear weighting schemes. A case study of 519 buildings showed that the *NEI*-enabled bi-objective analytics is automatic, effective, and inexpensive. Interviews with field experts confirmed that the analytics provides comprehensive evidence for a holistic identification of high-rise, high-density areas in need of nature exposure for landscape management and urban planning.

Keywords

Nature exposure; Window view; Walkability; Pareto optimality; 3D GIS; High-rise, high-density cities

Highlights

- Nature Exposure Index (*NEI*) defined on window views and walkability of natural sites
- Holistically assessed physical-visual nature exposures for the built environment
- Pareto optimality-based identification of areas with low-level nature exposures
- *NEI*-enabled analytics for probabilistic outputs and robustness of linear weightings
- A case study of a high-rise, high-density area with 519 buildings for validation

1 Introduction

Exposure to nature, such as greenery, sky, and waterbody, is preferred by urban dwellers because of well-recognized benefits for human physical and mental health, satisfaction, restoration, and productivity (Ulrich 1984; Kaplan 2001; Jiang et al. 2021). In contrast, less nature access in the urban context may exacerbate stress, depression, and other mood disorders (Ulrich 1984; Coppel & Wüstemann 2017). Given that almost all urban dwellers spend considerable time indoors, such as at home or working places (Andersen 2015), a convenient nature exposure from the neighborhood built environment is treasured.

Natural settings in the urban context are multi-faceted accessible resources for the built environment, particularly in high-rise, high-density cities with limited and fragmentally shared natural elements (Wolch et al. 2014). Visual and physical interactions are identified as two main ways of nature exposure (Keniger et al. 2013; Cox et al. 2017). Visually, natural elements from the urban landscape, e.g., greenery, water, and sky can be viewed through windows or balconies by urban dwellers. Physically accessible natural elements, embodied in green and blue spaces (e.g., parks and promenades), often scatter within the walkable range for daily outdoor activities. Nature exposures through the visual and physical pathways indicate inconsistent mediators for urban dwellers' embracement of nature.

Identification of the urban areas with both poor visual and physical exposures to nature, which is a multi-criteria decision analysis (MCDA) problem, can effectively facilitate smarter landscape management and urban planning (Choguill 2008; Xia et al. 2022). Nevertheless, traditional planning and design from individual perspectives often hinder a holistic analysis and allocation of the multi-faceted natural resources. For example, built environment and architectural design fields emphasize more on visual exposure to nature for buildings (CIBSE 2014; CEN/TC 169 2018), whereas urban planners underline the equal physical nature accessibility (Wolch et al. 2014; Tang et al. 2021). Researchers have developed many methods and urban indices to assess visual and physical nature exposures separately (Park & Guldmann 2020; Yang et al. 2021; Chen et al. 2022), but multi-faceted combinations were seldom considered. As a result, urban planners are often underinformed to balance multi-faceted natural resources. For instance, the buildings and blocks without any pathway of nature exposure, which should be preferential in urban renewal and revitalization, used to be unnoticed in traditional practices.

Recent geo-informatics technologies opened new avenues, such as 3D City Information Model (CIM) view imagery and walkability analyses, for a multi-faceted nature exposure extraction (Xue et al. 2021b). Deep learning models, e.g., Deeplab V3+ pretrained on *Cityscapes*, can be transferred to compute the nature view proportion in window view photos captured on 3D photorealistic CIMs (Li et al. 2022). The recent 3D pedestrian network has yielded opportunities for accurately assessing the walkability of nearby natural sites from residential buildings (Zhao et al. 2020; Tang et al. 2021). Bi-objective optimization of visual-physical nature exposures thus becomes technologically enabled especially in a multi-level 3D urban environment.

The research question of this study is thus:

"*How to assess and analyze the visual and physical facets of nature exposure holistically for identifying buildings and city blocks with both low values for a prioritized landscape management and urban planning?*"

To answer the question, we propose two objectives: i) to automatically assess floor-level visual and physical nature exposures for buildings, and city blocks in the 3D high-rise, high-density cities, and ii) to bridge the assessment results with decision-support analytics in landscape management and urban planning. This study first defines a two-dimension Nature Exposure Index (*NEI*) for multiple scales of the high-rise, high-density context by inclusively assessing both visual and physical exposures to nature. Thereafter, the *NEI*-based identification and prioritization of buildings and city blocks are formulated as a bi-objective optimization problem. An automatic Pareto optimality-based analytical method is adopted to identify buildings and blocks with low-level exposures to nature; and *NEI*-enabled analysis of linear weighting schemes can quantitatively examine the robustness of weightings and their probabilistic outputs for prioritization of the built environment improvement.

The main contribution of this study is three-fold.

i. From a theoretical perspective, this study defines a multi-dimensional *NEI* for representing urban dwellers' multi-faceted nature exposure. The multi-dimensional *NEI* enables holistic urban planning and analytics regarding visual and physical nature exposures. The multi-dimensional definition of *NEI* complements the existing studies, in particular in the 3D high-rise, high-density areas.
ii. From a methodological perspective, the automatic 3D assessment of *NEI* using the latest photorealistic window view imagery and 3D pedestrian network extends the conventional 2D modeling of nature exposure. *NEI*-based bi-objective analytics bridges the assessment results with decision-making in landscape management and urban planning.
iii. For practitioners, the bi-objective analytics of *NEI* offers a comprehensive and effective method for identifying buildings and blocks with unsatisfactory nature exposure. For conventional practices using linear weightings, the analytics can support planners' weight settings with outputs, probabilities, and robustness.

The remainder of this study is organized as follows. Section 2 reviews related work in the literature. Section 3 presents the definition of *NEI*, the automatic assessment of *NEI* using 3D GIS, and a set of *NEI* enabled bi-objective analytics. Section 4 describes a case study and the results. Sections 5 and 6 present the discussion and conclusion, respectively.

2 Literature review

2.1 Benefits and planning practices regarding exposure to nature

Numerous studies have been conducted to analyze the impact of exposure to nature on urban inhabitants, e.g., impacts on mental and physical well-being (Jiang et al. 2014; He et al. 2022). Visual exposure to nature is beneficial for physical and mental health. Window view as the main way to visually accessing nature is treasured by urban dwellers owing to their long-term indoor occupations (Cox et al. 2017). The benefits of the window views of nature include stress relief, attention restoration, and productivity promotion for urban dwellers (Ulrich 1984; Lottrup et al. 2015), which have been validated in multiple scenarios, such as residence, office, and hospital (Ulrich 1984; Kaplan 2001; Lottrup et al. 2015). By contrast, lacking views of nature may engender mental fatigue, stress, and more potential for violence (Kuo & Sullivan 2001).

Physical exposure through travels to nearby natural sites, such as natural parks, similarly, brings benefits to human health in terms of stress reduction (Hartig et al. 2014). High walkability of natural sites becomes increasingly important for residential buildings because it effectively encourages occupants to actively access nature, e.g., daily outdoor activities (Fan et al. 2017; Tang et al. 2021). More extensively, easy physical exposure to nature can also facilitate social cohesion, decrease crime rate, and revitalize the community (Lwin & Murayama 2011). By contrast, inconvenient physical nature exposure has shown a negative impact on urban dwellers' physical and mental health (Coppel & Wüstemann 2017; He et al. 2022).

Landscape management and urban planning have recently embraced narratives on the links between urban health and the benefits of exposure to nature (Wolch et al. 2014). Balancing the visual and physical nature exposures for buildings and city blocks becomes the main way for urban planners and designers to optimize natural resource allocation (Fisher-Gewirtzman 2018; Tang et al. 2021). For example, high-quality views of natural landscapes are considered in space planning of buildings and flats (USGBC 2019, p. 134; Laovisutthichai et al. 2021) and strategically shared in high-density urban environments (Fisher-Gewirtzman 2018), such as Hong Kong (HKTPB 2010). In addition, physical access to nature becomes important in urban regeneration and new town planning (Wolch et al. 2014). There is increasing policy interest in planning more neighborhood natural sites, such as parks, gardens, and ponds, to sustain urban health and livability (Raymond et al. 2016). Nevertheless, existing land constraints and relentless development pressures can hinder planners from simultaneously providing natural elements (e.g., greenery, water, and sky) for all buildings and blocks in need (Tang et al. 2021). Thus, identifying buildings and city blocks with both low-level visual and physical exposures to nature is a prerequisite of comprehensive orderly planning of natural resource settings for healthy high-rise, high-density urban development.

2.2 Quantified nature exposure measurement

Domain-isolated assessments of exposure to nature were studied from various perspectives for landscape management and urban planning. The quantification of visual exposure to nature utilizes visibility analysis (Fisher-Gewirtzman 2018) and view imagery (Helbich et al. 2019; Chen et al. 2022; Xue et al. 2021a) on the ground, floor, and overhead levels (Li et al. 2022). View collection has recently been transferred to the window level (Laovisutthichai et al. 2021; Li et al. 2021). Natural elements (e.g., greenery, water, and sky) of window view photos collected from 3D photorealistic CIMs can be automatically identified using a deep transfer learning model, e.g., Deeplab V3+ pre-trained on the *Cityscapes*, thereby providing opportunities to represent visual nature exposure of buildings and blocks in a multi-level urban environment (Li et al. 2022).

Physical accessibility has been measured using buffer zone, model-based, and distance-based assessment methods (Oh & Jeong 2007; Park & Guldmann 2020). For neighborhood services to function properly, walkability is often used to examine the connectivity between living and working places and nearby services, such as natural parks (Lwin & Murayama 2011; Tang et al. 2021). The recent reconstruction of a 3D pedestrian network with regard to topography and travel speed has enabled high accuracy of walkability measurement for physical nature exposure of buildings, particularly in high-rise, high-density cities (Sun et al. 2021; Tang et al. 2021).

Some emerging studies combined different forms of greenery exposure to understand the exposure disparity of urban areas comprehensively. For example, availability, physical accessibility, and eye-level visibility have been harmonized for greenspace exposure examination (Ye et al. 2019; Labib et al. 2021). However, existing nature exposure assessment methods encounter challenges in high-rise high-density urban environments. First, accessible nature by urban dwellers in high-rise, high-density cities cannot be represented by ground-level visibility (Li et al. 2022) and 2D accessibility (Zhao et al. 2020; Sun et al. 2021) of greenery. Furthermore, current integrated visual and physical assessments fail to bridge the multi-criteria decision-making process for prioritized improvement of the built environment. Thus, next-generation decision-support analytics for landscape management and urban planning should be able to examine multi-dimensional exposures to nature and identify buildings and city blocks with low-level visual-physical nature exposures for 3D high-rise, high-density cities, with up-to-date multi-criteria decision methods.

2.3 Multi-criteria decision analysis for urban planning

MCDA attempts to solve complex geospatial problems with multiple constraints, particularly for decision support applications (Malczewski 2006). In general, MCDA comprises two categories: multi-attribute decision analysis and multi-objective optimization. Compared to the multi-attribute decision analysis returning a single result, multi-objective optimization outputs multiple results for a set of specific objectives (Malczewski & Rinner 2015), enabling a comparison for planners' final decisions. Pareto optimality is one of the cornerstone concepts of multi-objective optimization that attempts to identify all non-dominated results as Pareto-optimal solutions (Huang et al. 2008; Malczewski & Rinner 2015). This concept has been used in typical multiple objective scenarios, such as land use allocation and urban infrastructure site planning (Huang et al. 2008; Rahman & Szabó 2021). Thus, Pareto optimality-based optimization can be used to identify a set of solutions for bi-objective analytics of 3D visual-physical exposures to nature in high-rise, high-density cities.

In summary, the targeted bi-objective optimization analytics of 3D visual-physical nature exposures in this paper is a research gap to close in landscape management and urban planning studies. Among the reasons are the previous immature 3D visual-physical representations (e.g., window views and walkability) of nature exposures in high-rise, high-density cities, and the minimal consideration in their integrated assessment and analytics for comprehensive decision-making in landscape management and urban planning. Meanwhile, automatic deep transfer learning-based window view assessment, 3D pedestrian network analysis, and Pareto optimality-based optimization may provide opportunities to advance the automatic multi-dimensional nature exposure analytics for significantly improving the visual-physical nature exposures of the built environment in high-rise, high-density cities.

3 Research methods

Figure 1 shows the conceptual framework of the proposed *NEI* and related analytics. In general, 3D data inputs comprise photorealistic CIM and building footprints for window view measurement, as well as pedestrian network, floor sites, and natural site entries for the physical accessibility. The proposed automatic integrated nature exposure assessment and analytical methods for prioritized built environment improvement consists of two parts: (i) *NEI* definition together with the automatic floor-level visual-physical nature exposure assessment and (ii) Bi-objective optimization-based analytics of *NEI*. The final output includes three parts: buildings or blocks with both low-level nature exposures, probabilistic outputs of linear weightings, and robustness of target weighting for an invariant output.

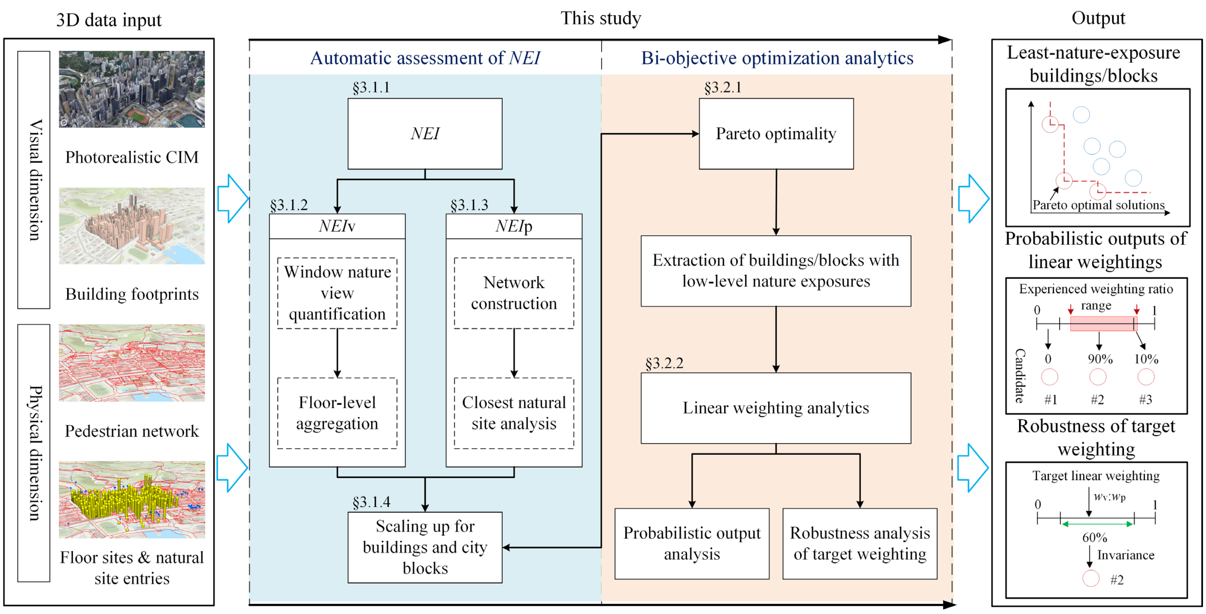

Figure 1. Conceptual framework of the proposed *NEI* and bi-objective analytics.

3.1 Automatic assessment of *NEI*

3.1.1 General definition of NEI

Given a floor of a building in the built environment, *NEI* is a two-dimension vector:

$$NEI = (NEI_v, NEI_p), \tag{1}$$

$$NEI_v = (FNVI - FNVI_{min}) / (FNVI_{max} - FNVI_{min}) \in [0, 1], \tag{2}$$

$$NEI_p = (t_{max} - t) / (t_{max} - t_{min}) \in [0, 1], \tag{3}$$

where NEI_v denotes a relative floor-level visible nature proportion in an area, *FNVI* represents an absolute nature view proportion of a floor, and $FNVI_{min}$ and $FNVI_{max}$ are the maximum and minimum values of *FNVI* in the context area. In addition, NEI_p is the physical component representing the relative walkability from the floor to the nearest natural site (e.g., nature parks and seaside) in the area. Considering the set of walking time t for all floors in the context area, NEI_p is denoted as a normalized value computed by t, t_{max}, and t_{min}. Thus, both NEI_v and NEI_p are scalars bounded between 0 and 1, and the closer to 1 they are, the higher levels of visual and physical nature exposures the floor owns.

Given a two-dimension vector of weighting $w = (w_v, w_p)$, where $w_v + w_p = 1$, the weighted sum of an *NEI* is a scalar:

$$wNEI = NEI \times w^T \in [0, 1], \quad (4)$$

where w_v and w_p represent the weighting values for NEI_v and NEI_p, respectively. Moreover, w used to be set by experts or statistics from surveys. For example, an equal weighting pair $w = (0.5, 0.5)$ indicates the equal significance of visual and physical exposures to nature. A small *wNEI* value indicates the inconvenience of daily access to nature, thereby deserving a high priority for the renewal and revitalization in the context area.

3.1.2 The visual component of NEI

This study defines NEI_v using the average visible nature proportions of window view photos captured at the floor level. Given a virtual view photo captured on a window of the 3D photorealistic CIM, WVI_α defined in (Li et al. 2022) presents the ratio of visible greenery, waterbody, and sky:

$$WVI_\alpha = \text{Number of pixels in } \alpha \,/\, \text{Total pixels of the view photo}, \ \alpha \in \{\text{greenery, waterbody, sky}\}. \quad (5)$$

Regarding greenery, water, and sky as visible natural elements, we first summarize the *FNVI* from WVI_α of floor-level window view photos. More specifically, assuming m view photos captured on the different facades of a floor, *FNVI* is calculated from WVI_α^i ($i = 1, 2, 3, \ldots, m$) with the sampling interval I_i as weights as shown in Eq. 6. Last, NEI_v is computed as an output using *FNVI*, $FNVI_{min}$, and $FNVI_{max}$.

$$FNVI = \textstyle\sum_{i=1,\ldots,m} (WVI_\alpha^i \times I_i) \,/\, \textstyle\sum_{i=1,\ldots,m} I_i. \quad (6)$$

Figure 2 shows the workflow consisting of view site sampling, view generation, and deep transfer learning-based computing of WVI_α. We compute the modeled NEI_v on 3D photorealistic CIMs instead of physical sites, as shown in Figure 2a. Li's (2022) method is utilized to automate the photorealistic window view quantification as shown in Figure 2b. We first apply an even sampling method to ensure at least two view sites for individual facades of a floor (max $I_i = 20$ m). Then, a virtual camera with a 60-degree field of view (Tara et al. 2021; Li et al. 2022) is set on the designated sites of CIMs to capture the window view outside. A deep transfer learning model, DeepLab V3+ trained on the *Cityscapes* with a machine-learning classifier helps segment the window view photo for nature view quantification. In the end, sample window view photos on the same floor of the building are aggregated to summarize WVI_α^i for NEI_v, as shown in Figure 2c. 3D locations and their floor and building IDs are geo-tagged to the NEI_v datasets.

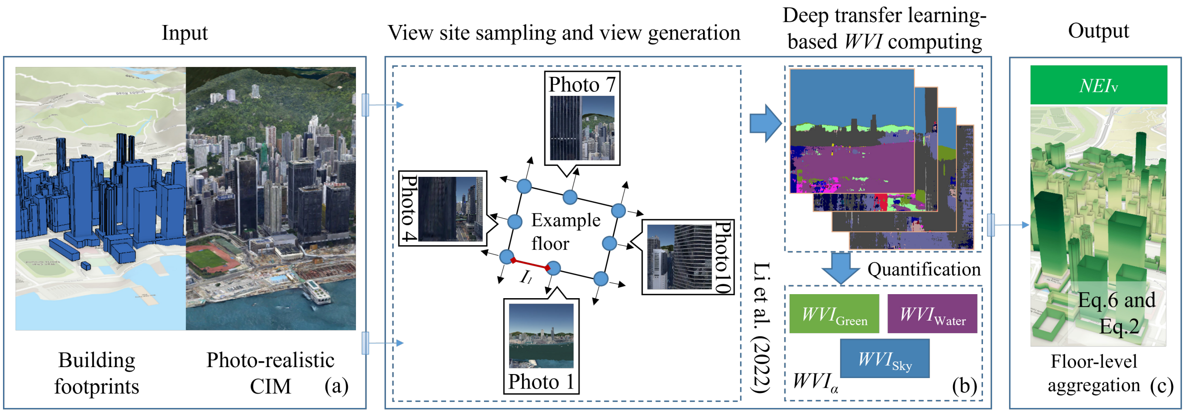

Figure 2. Deep transfer learning-based estimation workflow for NEI_v.

3.1.3 The physical component of NEI

NEI_p is modeled using walking time from the occupant's building floor to the entry of the nearby natural site through the shortest path *S*. Natural sites in this study include parks, gardens, and promenades, which are dominantly covered or surrounded by natural elements, such as vegetation and waterbody to serve outdoor activities and recreation. Within the high-rise, high-density context, we connect the staircase and lift of buildings with exterior pedestrian urban fabrics, thereby updating a more comprehensive and computable 3D urban system. Meanwhile, pedestrian walking speed is different on walkway types, such as the path of different slopes, transport systems, and interference like crossing and traffic islands. Thus, S is divided into n segments $s_1, s_2, \ldots, s_n$, where the corresponding walking speeds are v_1, $v_2, \ldots, v_n$. The walking time t is computed as the sum of the n quotients as follows:

$$t = \sum\nolimits_{i = 1, \ldots, n} d\,(s_i) / v_i, \qquad (7)$$

where d is a function to calculate the distance of s_i. Last, NEI_p is computed by t, $t_{\min}$, and $t_{\max}$.

We compute the NEI_p from the simulated walking through a 3D pedestrian network, consisting of interconnected path segments, such as lifts, staircases, sidewalks, and footpaths. We measure the closest natural site to compute NEI_p. 3D building floor sites and natural site entries are set as origins and destinations, respectively, as shown in Figure 3. Within the interior buildings, lifts and staircases are used to simulate the walking situation. Travel distance by lift is considered the vertical distance between the floor and ground levels, while staircase length is assumed as the vertical distance divided by sin 35° (HKLWB 2006).

Walking speed v_i of different walkway types is added to the 3D pedestrian network following the field tests of normal adults, previous studies, and regulations (Oh & Jeong 2007; Tang et al. 2021; HKBA 2011). Urban planners and researchers can finetune the control parameters for specific application scenarios.

$$v_i = \begin{cases} 100e^{-3.5|\tan\theta+0.05|}, & \text{type}(s_i) \in \text{Footpath} \\ 120, & \text{type}(s_i) = \text{Travellator} \\ 105, & \text{type}(s_i) = \text{Lift} \\ 48, & \text{type}(s_i) = \text{Escalator} \\ 39, & \text{type}(s_i) = \text{Staircase} \\ 6, & \text{type}(s_i) \in \text{Interference} \end{cases}, \tag{8}$$

where v_i is measured in meters per minute, Footpath = {Footway, footbridge, service lane, ramp, generalized walkway, underpass} is the set of paths with different slopes, and Interference = {Crossing, traffic island} is the set of places where pedestrians need to wait to cross the street. Tobler's hiking function (Tobler 1993) is used to simulate slope impact on walking speed. The slope θ is positive for walking uphill and negative for walking downhill. Last, the value of t is computed by combining all the time consumed on the segments of the shortest path and NEI_p is computed using t, t_{max}, and t_{min} (see Figure 3). Values of NEI_p are saved with the corresponding 3D locations and floor and building IDs.

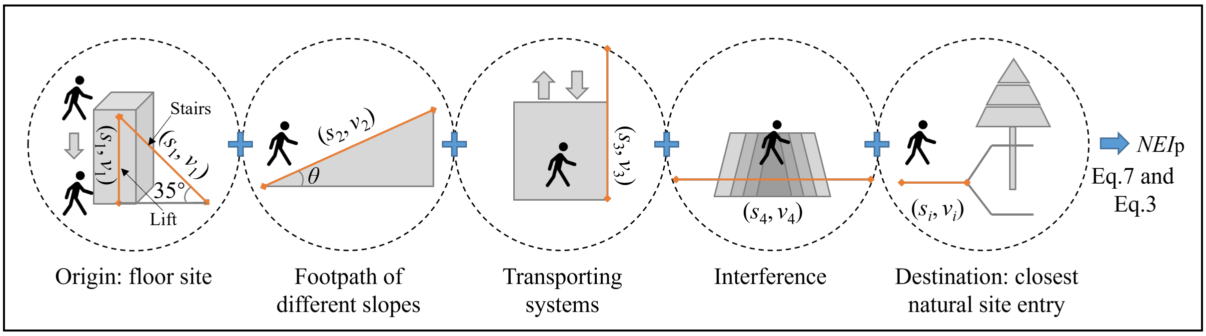

Figure 3. NEI_p computing based on the pedestrian network analysis

3.1.4 Scaling up for buildings and city blocks

Modern landscape management and urban planning aim to improve nature exposure to the built environment through active intervention, such as planning more parks, roof gardens, and vertical greenery. Moreover, buildings and blocks are the main analytical units in measuring nature exposure to help priority identification. For fulfilling urban planners' needs, floor-level datasets can be adaptively aggregated into corresponding buildings and blocks based on building IDs and topological relationships. For example, at the building level, NEI_{v} sets with the same building IDs are considered as a group and the $NEI_{\mathrm{v\_bldg}}$ is computed as a floor-area-based linear weighted sum.

3.2 Bi-objective optimization-based analytics of *NEI*

3.2.1 Pareto optimality for identifying least-nature-exposure areas

An *NEI*-based MCDA is a bi-objective optimization problem. Pareto optimality is used to identify all potential areas with both low-level exposures to nature. For example, the search of buildings with low-level visual-physical nature exposures can be formulated as:

$$P = \arg\min_{x \in X} NEI_{\mathrm{bldg}}(x), \tag{9}$$

where X is the set of buildings x in the planning area, as shown in Figure 4a. Figure 4b shows that Pareto optimal building set $P \in X$ is the set of non-dominated buildings x^* in terms of least NEI_{bldg}. Any rest building, i.e., in $X \setminus P$, have both $NEI_{\mathrm{v\_bldg}}$ and $NEI_{\mathrm{p\_bldg}}$ greater than at least one Pareto optimal building x^* in P:

$$P = \{x^* \mid \neg \exists x \in X, NEI_{\mathrm{v\_bldg}}(x) \le NEI_{\mathrm{v\_bldg}}(x^*) \text{ and } NEI_{\mathrm{p\_bldg}}(x) \le NEI_{\mathrm{p\_bldg}}(x^*)\}. \tag{10}$$

Thus, by excluding dominated buildings ($X \setminus P$), the Pareto optimal buildings x^* of P become the least-nature-exposure candidates for the prioritized improvement. In practice, a buffer zone of Pareto front constructed by P, as shown in Figure 4b, can also be set to involve more buildings with near-low-level visual-physical nature exposures (e.g., building #1) for more inclusive consideration.

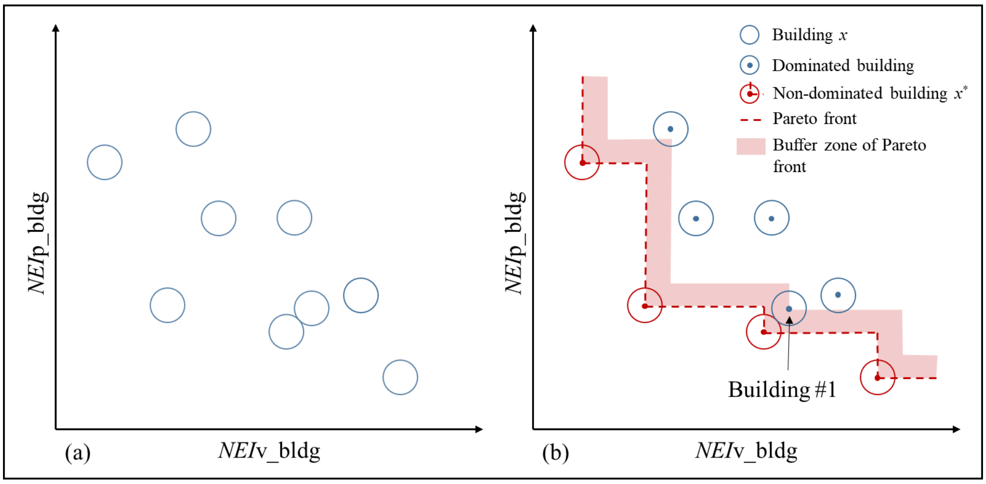

Figure 4. Identification of the Pareto optimal buildings. (a) Example buildings X, and (b) Pareto optimal building set P visualized in the plot of $NEI_{\mathrm{v\_bldg}}$ and $NEI_{\mathrm{p\_bldg}}$.

3.2.2 Linear weighting analysis for probabilistic outputs and robustness

We present a linear weighting analysis to decipher the relationship between weightings and the final output from P. In traditional practices, urban planners employ linear weightings from various scientific assumptions (e.g., expert knowledge and statistics) to integrate multiple indices for a final output, where planners are often puzzled by various weightings due to varied strengths and weaknesses. The presented analysis involves all the recommended weightings at one time and returns the probabilistic outputs and robustness of linear weightings.

Figure 5 shows that a fixed linear weighting represents a set of straight parallel lines with a determined slope. For example, weighting pair $w = (0.5, 0.5)$ represents parallel lines with the slope $k = -w_{\mathrm{v}} / w_{\mathrm{p}} = -1$ passing Pareto optimal building points. The closer the line to the origin, the lower the level of $wNEI$ the building access. When the weighting ratio k changes, the convex point with the lowest $wNEI$ may change, i.e., C_1, C_2, and C_3, as shown in Figure 5b. Isoline with the lowest $wNEI$ reaches the same convex point(s) on the Pareto front when k changes within the ranges of A_1, A_2, or A_3 in blue. The relationship between the output and the weighting ratio $k = -w_{\mathrm{v}} / w_{\mathrm{p}}$ is shown in Eq. 11.

$$C = \begin{cases} C_1,\ k \in A_1 = (-\infty, k_1] \\ C_i,\ k \in A_i = [k_i, k_{i+1}],\ 1 \le i \le N-1. \\ C_N,\ k \in A_N = [k_N, 0] \end{cases} \tag{11}$$

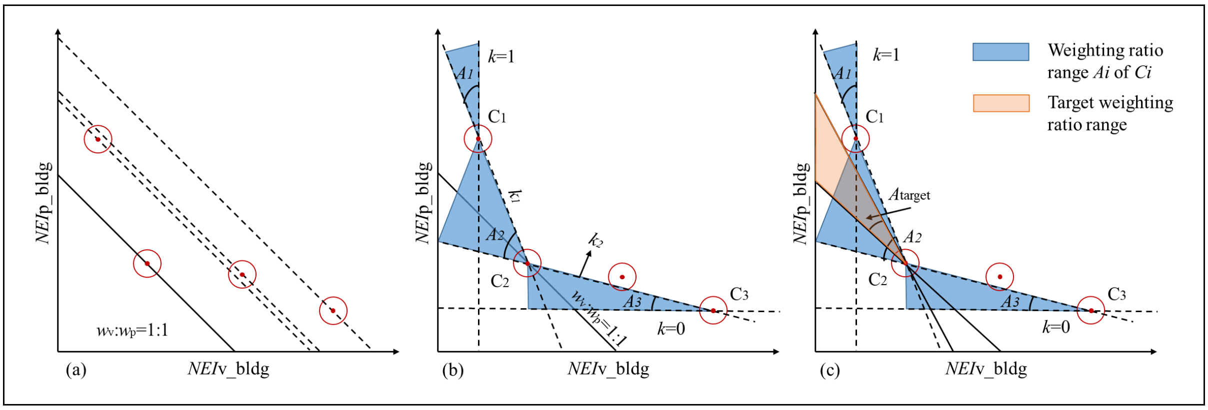

Figure 5. Analysis of linear weighting schemes. (a) Parallel lines indicating equal weightings, (b) relationship between weightings and outputs, and (c) least *NEI* building identification by overlapping the target range to the weighting ratio range of *C*.

When the recommended weightings are in a range and not finally determined, urban planners can directly use the range A_{target} as the input in Figure 5c. Then, the probability of any candidate C_i is measured using the overlap between A_i and A_{target}:

$$\text{Probability}\ (C_i) = rad\ (A_i \cap A_{\text{target}}) / rad\ (A_{\text{target}}), \tag{12}$$

where *rad* is a function to compute the radian of A. For example, Figure 5c indicates that the A_{target} is a subset of A_2. Thus, considering all the weightings, the candidate building C_2 is always the final output, with probability = 100%. In addition, the robustness of target weighting for an invariant final output can also be assessed. Eq. 13 shows the robustness of target weighting ratio k is computed based on the corresponding radian of A_i. For example, the target weighting pair, $w = (w_v, w_p)$, $k = -w_v / w_p = -1$ within A_2, as shown in Figure 5b, owns a robustness, $rad(A_2)/0.5\pi$, to ensure the invariance of the final output C_2.

$$\text{Robustness}\ (w) = rad(A_i)/0.5\pi,\ k = -w_v / w_p \in A_i. \tag{13}$$

4. Case study

4.1 Study area and settings

The study area includes a total of 519 buildings in 57 town blocks of Wan Chai, one of the most high-rise, high-density areas in Hong Kong (HKPlanD 2018), as shown in Figure 6. The average building height is 35.5 m and the maximum plot ratio is 10.0. Major natural elements, e.g., vegetation and water from mountains and sea, are located in the northern and southern areas, while the minor scatters in parks and gardens. Because of the vertical development and imbalanced natural settings, the occupants in the case area encounter considerably different visual and physical nature exposures, the variance of which is confirmed in Sections 4.2.1 and 4.2.2.

Building footprints with height information were extracted from the iB1000 digital map of Hong Kong (HKLandsD 2014), as shown in Figure 6c, while a 3D photorealistic CIM was from the Planning Department (2019). For physical accessibility, the 3D entry points of case natural sites in blue were collected from the Leisure and Cultural Services Department of Hong Kong and Google Map in Figure 6e, while the 3D pedestrian network in red was from the Lands Department (HKLandsD 2021). Moreover, the number of stories of buildings in yellow and lift information were extracted from the Home Affairs Department (HKHAD 2021) and Electrical and Mechanical Services Department (HKEMSD 2021), respectively.

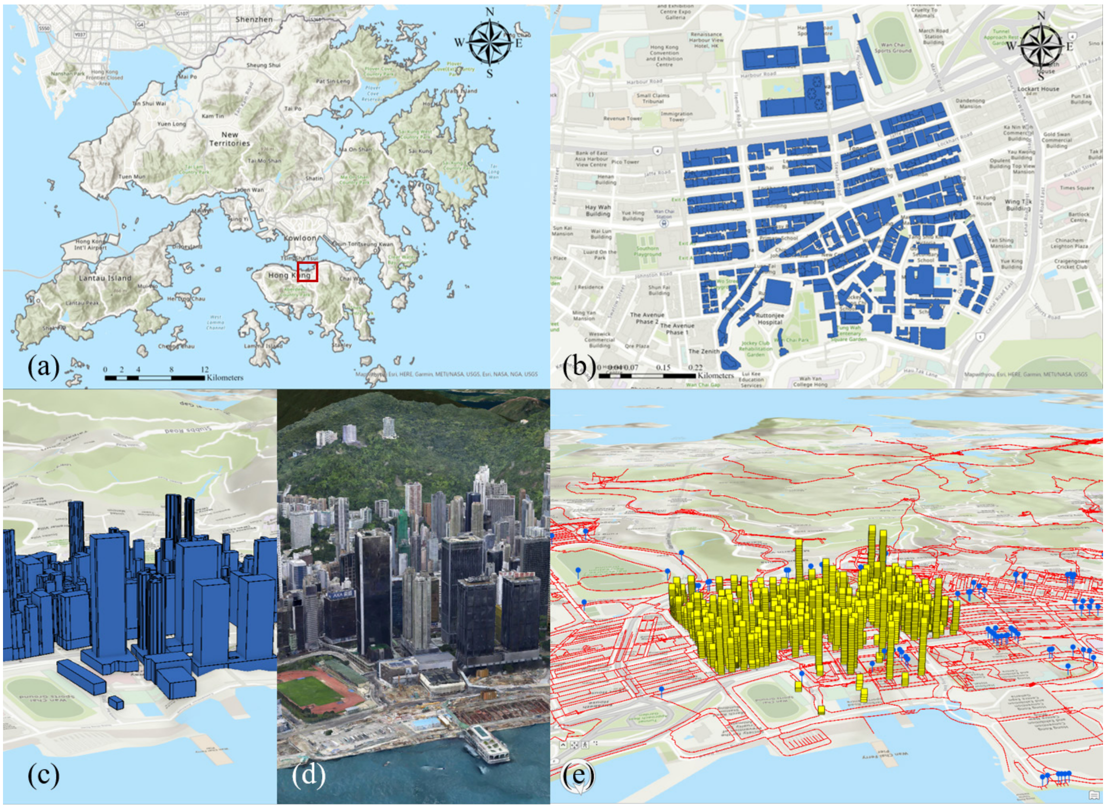

Figure 6. Study area of Wan Chai, Hong Kong. (a) Location, (b) 519 buildings, (c) building footprints and heights, (d) CIM, and (e) 3D pedestrian network with floors and entry points.

The computational process was set up as follows. This study used a workstation with an Intel i7-10700 CPU (2.90GHz, 16 cores), 128 GB memory, one NVIDIA GeForce RTX 2070 graphic card, and Windows 10 and Ubuntu 20.04 dual system (64-bit). Floor-level window views were generated with the Cesium (ver. 1.75), a software platform for processing and visualization of 3D geospatial data. We adopt Li's (2022) deep transfer learning-based window view quantification with the environment of Tensorflow (ver. 2.4), Python (ver. 3.6), and Orange 3 (ver. 3.26, a Python machine learning platform). The NEI_p measurement and multi-scale spatial pattern visualization were implemented with ArcGIS Pro (ver. 2.7.3). Last, Pareto optimality-based bi-objective optimization analytics was implemented through a decision support tool developed on the ArcGIS Pro platform.

4.2 Results

Table 1 lists the time cost of all the steps in the case study. The full assessment and analytical process was completed within 21.37 hours. The window view quantification consumed > 99.9% of the processing time, while all rest steps consumed < 62 s in total. The accuracy of NEI_v was satisfactory ($R^2 > 0.95$) according to Li et al. (2022), while the accuracy of NEI_p was confirmed (RMSE < 0.12) by a normal adult through field tests.

Table 1. Computational time of the proposed automatic assessment and analytical method.

Ref. sect.	Variable to produce	Processing	Software library	Total time
3.1.2	NEI_v	View quantification (Li et al. 2022)	Cesium, Deeplab V3+, and Orange 3	21.35 h
		Floor-level aggregation	ArcGIS Pro	2.62 s
3.1.3	NEI_p	Closest natural site analysis	ArcGIS Pro	58.16 s
3.1.4	NEI_{bldg}	Building-level aggregation	ArcGIS Pro	0.63 s
3.2.1	P	Pareto optimality-based optimization	ArcGIS Pro	0.52 s
3.2.2	$wNEI$	Linear weighting analysis	ArcGIS Pro	0.01 s
			Total	21.37 h

4.2.1 Floor-level results

NEI_v and NEI_p were computed and visualized on the 3D building footprints, as shown in Figure 7. Figure 7a shows upper building floors often enjoyed high-level nature views, while inland lower building floors were with less visual exposure to nature. Although some floors could have a high-level nature view ($FNVI = 0.62$), there still existed floors with no visual nature exposure. Meanwhile, Figure 7b shows buildings surrounded by natural sites tended to own better convenience for physical access. By contrast, building floors in the lighter color indicated lower accessibility, in which the maximum t was above 10 min.

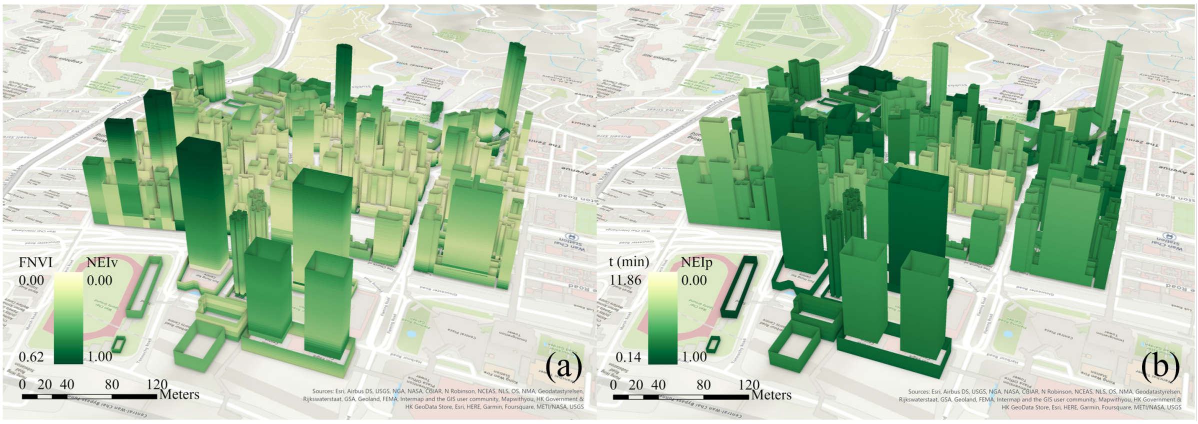

Figure 7. Disparity of exposures to nature. (a) NEI_v and (b) NEI_p.

The box plots in Figure 8 suggest that the holistic nature view acquisition of the building floors in this area was not high, where the median value of *FNVI* was approximately 0.16. One-fourth of the building floors were without exposure to nature (*FNVI* < 0.1) due to compact surrounding construction elements. Meanwhile, the median t was approximately 4.5 mins, with a distribution from 0.14 to 11.86 mins. Travel time from at least one-fourth of the building floors to the closest natural site was longer than 5.7 mins. As shown in Figure 8c, NEI_v nearly had an ignorable negative correlation with NEI_p (Spearman's coefficient $\rho = -0.149$, $p \leq 0.0001$). The ignorable correlation also indicated that it is necessary to use an integrated assessment for a more comprehensive understanding of exposure to nature in the case area.

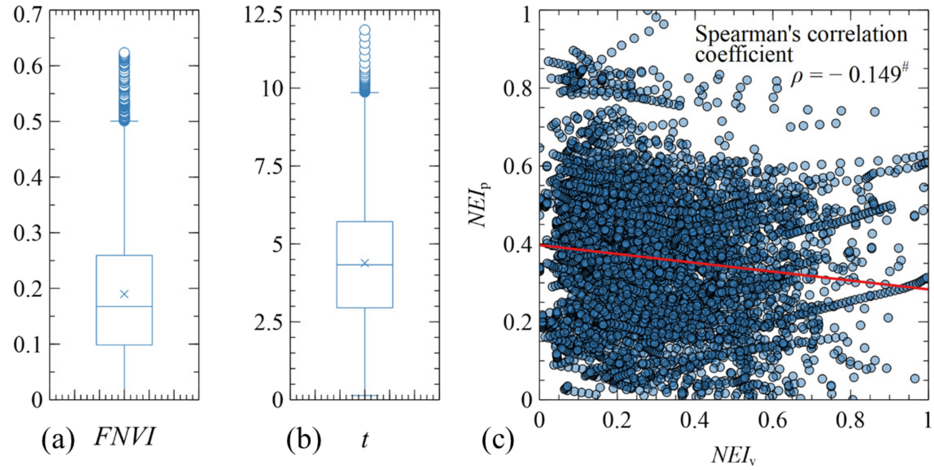

Figure 8. Statistical results. Box plots for (a) *FNVI* and (b) t, and (c) Spearman's correlation coefficient of NEI_v and NEI_p (#: two-tailed significance $p \leq 0.0001$).

4.2.2 Building-level results

Figure 9 shows spatial patterns of NEI_{v_bldg} and NEI_{p_bldg}. The distribution of NEI_{v_bldg} was found to be discrete. Through the validation from 3D photorealistic CIM, unobstructed buildings nearby the hills, artificial greenery, or seaside, as shown in circles #1 and #2, tended to have a better nature view acquisition. By contrast, the spatial distribution of NEI_{p_bldg} was more clustered. For example, buildings in red circle #3 had higher NEI_{p_bldg}, whereas NEI_{p_bldg} of buildings in circle #4 was lower. Observation of CIM showed that buildings in circle #3 owned a close-range park in the surrounding environment, while there only existed surrounded construction elements for the buildings in circle #4. That is, the current natural resource setting has led to an evident disparity of visual and physical nature acquisitions for urban dwellers in the context area.

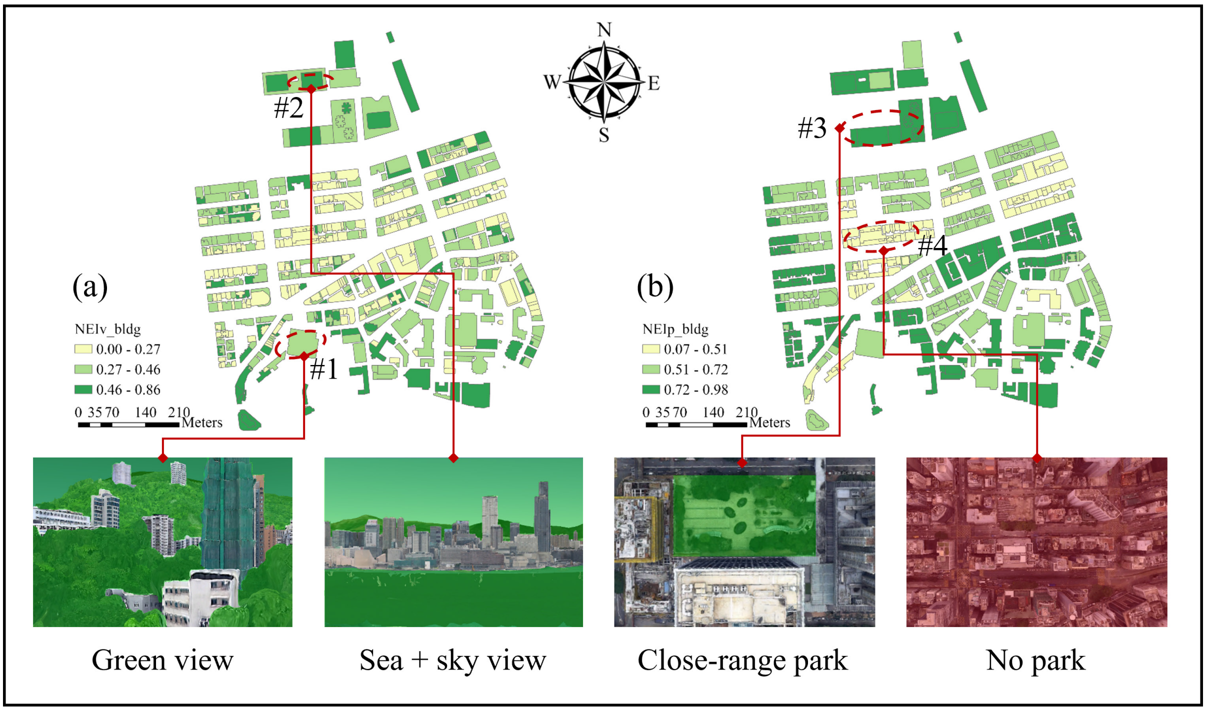

Figure 9. Building-level results with observational validation. (a) NEI_{v_bldg} and (b) NEI_{p_bldg}.

4.2.3 Automatic identification of least-nature-exposure areas for urban planning

The building-level analytics was implemented as a user-friendly add-on on the ArcGIS platform, as shown in Figure 10. A user can input NEI_{v_bldg} and NEI_{p_bldg} in Section 4.2.2, as well as the buffer zone of the Pareto front, acceptable weighting range, and target weighting pair for robustness analysis, as shown in Figure 10b. Note that representations of a weighting pair (w_v, w_p), e.g., “0.25, 0.75” and its ratio “0.33” are both acceptable for the inputs. The analytics outputs comprised three parts: (i) Pareto optimal buildings, namely, the set of buildings with both low-level visual and physical nature exposures; (ii) probabilistic outputs according to acceptable linear weightings; and (iii) robustness of the target weighting for an invariant output.

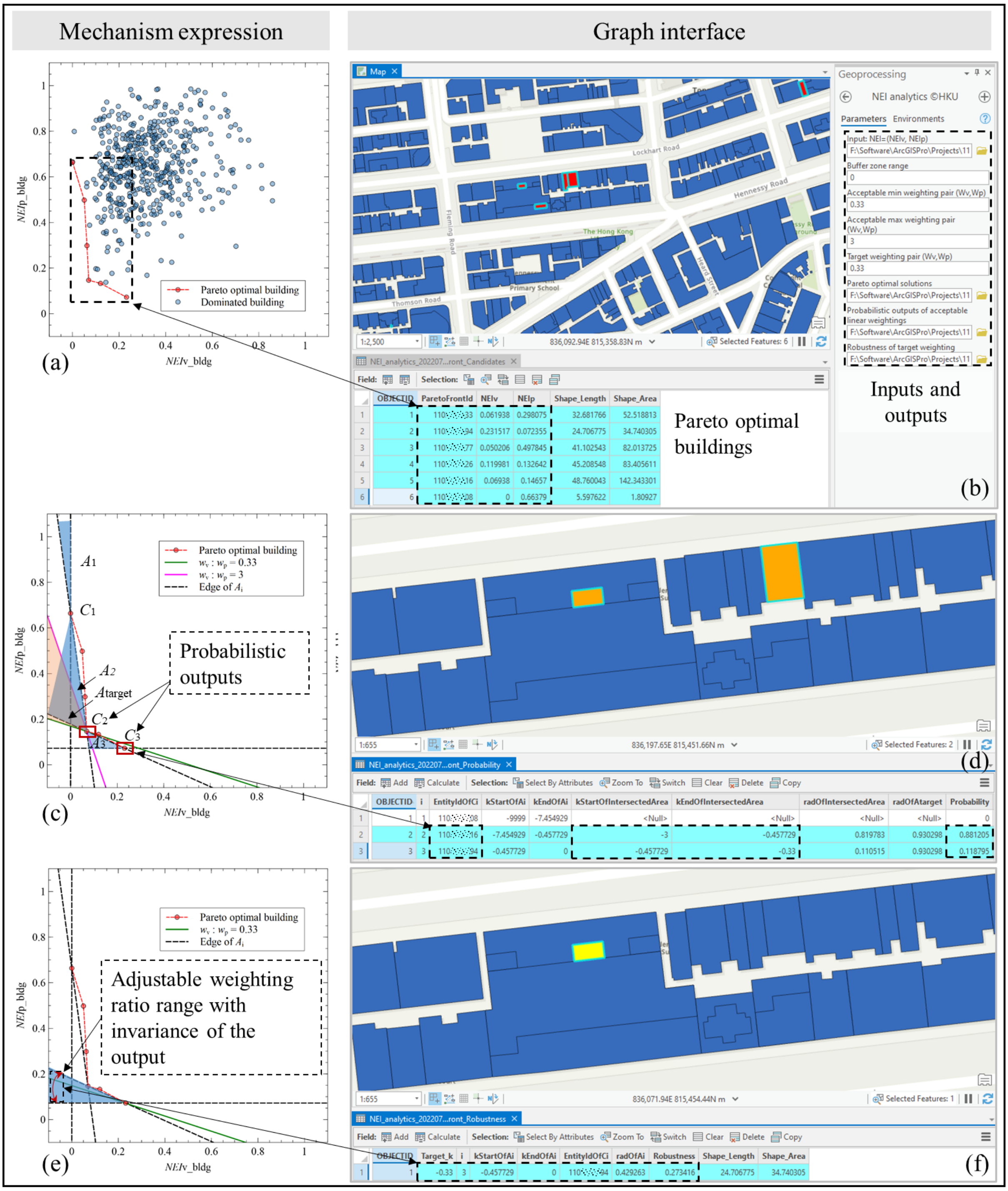

Figure 10. Results of automatic identification. (a) Pareto optimal buildings, (b) *NEI*-based building query through an ArcGIS addon, (c) two probabilistic output buildings from a range of linear weightings, (d) results of probabilities in the addon, (e) robustness of a target

weighting for an invariant output, and (f) results of robustness in the addon.

The Pareto optimal solutions included six buildings with the least *NEI*s using exhaustive Pareto optimality-based bi-objective optimization (buffer zone range = 0), as shown in Figures 10a and 10b. No other buildings could have poorer visual and physical nature exposures than the six in red in Figure 10a. Figures 10c and 10d show the probabilistic buildings under a target linear weighting ratio range—from $w_v : w_p = 0.33$ to 3 set by users. Only two buildings were possible to be the final outputs because A_{target} covered two weighting ratio ranges (i.e., A_2 and A_3) as shown in Figure 10c. Figure 10d shows building #110***16 was selected when the weight ratio ranged between 0.46 and 3, while building #110***94 represented the ratio from 0.33 to 0.46. Within the acceptable weighting ratio range, building #110***16 had a higher possibility (88.12%) to be considered as the final output. By contrast, concave points on the Pareto front, such as building #110***08, had zero possibility of being selected when using the acceptable weight ratio range, though they also owned low-level visual-physical nature exposures. Table 2 details the values of *wNEI* for two probabilistic buildings using the acceptable maximum and minimum weighting pairs.

Table 2. List of probabilistic buildings for the acceptable weighting ratio range.

No.	Building ID	Weighting pair (w_v, w_p)	Least *wNEI*
1	110***16	(0.75, 0.25)	0.09
2	110***94	(0.25, 0.75)	0.11

Figures 10e and 10f show the robustness analysis of a target weighting ratio $w_v : w_q = 0.33$. The robustness of the weighting ratio $w_v : w_q = 0.33$ was 27.34% to ensure invariance of the output (i.e., building #110***94) using Eq. 13. In summary, the in-house developed ArcGIS add-on can effectively guide a user to examine buildings' *NEIs*, list the probabilistic outputs, present robustness of a linear weighting, and support explainable decision-making processes.

4.2.4 Comments from domain experts

Four domain experts were interviewed independently to validate and evaluate the proposed method. Two experts are professors of landscape management, while the other two are urban planners working at planning and redevelopment authorities. Before asking questions in the interviews, we introduced and demonstrated *NEI* and the analytical results through the case study. The two professors emphasized the integrated 3D quantification of the exposure to nature in the vertical metropolis and compared the fixed weight setting method with the Pareto optimality-based bi-objective analytics, respectively:

> Professor A: "It is promising for guiding urban landscape management and planning, especially in high-rise, high-density cities. The integrated 3D nature exposure assessment is more comprehensive and effective for understanding the multi-level urban environment."

> Professor B: "Expert knowledge is often used to determine the weight setting. Pareto optimality-based bi-objective optimization method and the linear weighting analysis can identify all the building candidates and explain the possible outputs."

In the end, both professors suggested that the view is "rather complex than a simple proportional indicator." Views can be "further quantified from in-depth perspectives such as view structure in the future."

In comparison, the two planners focused on the potential scenarios and availability for decision-making:

> Planner C: "It allows the user to better understand the data relationship, and thus minimizes the data size to be studied. The full picture between the linear weightings and probabilistic outputs gives us a much clearer understanding and decision-making space."

> Planner D: "It can effectively provide insights on how to enhance the site selection process for urban renewal, and to my best knowledge, no bi-objective optimization-based analytics was utilized to help the identification of buildings and blocks in need of nature exposure."

Although it is promising and practical to identify the "first-needed" area with comprehensive evidence, both suggested other indicators, such as building condition, to supplement *NEI* for more comprehensive decision-making in urban redevelopment and preservation.

In general, both disciplines of experts confirmed that the proposed method was promising for guiding landscape management and urban planning. First, the integrated 3D nature exposure assessment is markedly comprehensive and effective for understanding the multi-level urban environment. The proposed analytics can narrow the focus scope, identify all building candidates with low-level visual-physical exposures to nature, and explain the probabilistic outputs of linear weightings. As far as they were concerned, no bi-objective optimization-based analytics was available for identifications of buildings and blocks with low-level visual-physical exposures to nature. In terms of applicability, all experts agreed that the Pareto optimality-based bi-objective decision support tool could effectively help inform decision-making in both disciplines.

5 Discussion

5.1 Significance

From a theoretical perspective, the proposed visual-physical *NEI* definition extends the existing studies on isolated nature exposure measurement to an integrated examination process. The *NEI* enables and advocates holistic urban planning and analytics for multi-dimensional nature exposures. Integrated analytics of visual-nature nature exposures for buildings and city blocks is significant in improving the current urban planning paradigm in the high-rise, high-density cities.

From a methodological perspective, an integrated 3D assessment of visual and physical exposures to nature effectively examines the disparity of natural resource possession in the multi-level urban environment. *NEI*-based bi-objective analytics bridges the assessment results with decision-making in landscape management and urban planning. The proposed Pareto optimality-based optimization method can ensure all the buildings and blocks with low-level visual and physical nature exposures are identified at one time, thereby offering an entire picture of the focus scope.

For practitioners, the proposed method is easy to use and low-cost. Assessment methods can automatically identify buildings and blocks with low-level visual-physical nature exposures from holistic perspectives. The analytical results of prioritization of buildings for improvement in visual-physical nature exposures are comprehensive and explainable with the possible linear weighting schemes. Accordingly, urban planners and other decision-makers are enabled to make a well-informed determination with quantified evidence. In summary, the proposed method contributes an integrated visual-physical nature exposure assessment using CIM and pedestrian network, and thus provides a low-cost and highly explainable analytical tool for landscape management and urban planning.

5.2 Limitations and future work

This study has several limitations. First, NEI_v and NEI_p in this paper involve neither window settings nor personalized travel preferences. Thus, NEI_v modeled on the photorealistic CIM can be extended to represent window settings such as grills and scales through Building Information Modeling, while NEI_p can be personalized by path weighting, such as a 50% "psychological" discount on walking time for a clean, familiar, and safe path environment. Another future research direction is integrating other representations of exposure to nature, e.g., incidental nature interactions on the streets and inverse representation of acoustic nature exposure, such as urban noise. Moreover, urban planners and landscape architects need to review the exposure suggestions with other indicators, such as availability of lands, maintenance costs, and social concern, to determine the final objectives for improvement of the built environment. Another future endeavor is to incorporate related indicators and turn the proposed bi-objective optimization analytics into a multi-objective decision-making. Besides, despite the acceptable time cost of Pareto optimality-based bi-objective analytics, the NEI_v computing process is still time-consuming owing to the generation and segmentation of view photos. Thus, given that the proposed definition is compatible with various window view quantification techniques, more efficient methods will be useful. Last, the aggregation of human-level assessment results of nature exposure into buildings and blocks can be more accurate than the floor-level one in this study, which can be another direction to advance fine-scale nature exposure modeling in future landscape management and urban planning.

6 Conclusion

Natural settings in the urban context are multi-faceted resources for urban dwellers. A holistic visual-physical nature exposure assessment is needed for improving the built environment. Traditional assessment often focuses on either visual or physical dimension in isolation, and thus fails to identify the buildings and blocks with both low visual and physical nature exposures.

This study defines a Nature Exposure Index (*NEI*) that has both visual and physical components. Thereafter, *NEI* is measured through floor-level window views and walkability of nearby natural sites. By aggregating the results into building or block levels, a bi-objective optimization-based analytics is presented to identify areas with the least visual-physical nature exposures. Last, probabilistic output buildings or blocks and robustness of linear weightings are gauged through a linear weighting analysis. Our method achieved a satisfactory result for a pilot study of 519 buildings in the high-rise, high-density area of Wan

Chai in Hong Kong. Comments from experts and planners indicated that the proposed method is effective and applicable for better landscape management and urban planning.

The proposed method is automatic, effective, and scalable up to buildings and city blocks. The assessment results of *NEI* represent a full picture of visual-physical nature exposures. The analytical results of Pareto optimality and weighting analysis enable a holistic and in-depth understanding of the buildings and city blocks that need improvement in visual-physical exposures to nature. Future directions include in-depth and comprehensive visual-physical nature exposure examination, more efficient view quantification methods, human-level analytics of nature exposure, and incorporating related indicators to the presented addon for a decision-making system.

Acknowledgment

This study was supported in part by the Hong Kong Research Grant Council (RGC) (Nos. T22-504/21-R, 27200520) and Guangdong-Hong Kong-Macau Joint Laboratory for Smart Cities of the 2020 Guangdong New Innovative Strategic Research Fund, Guangdong Science and Technology Department (Project No.: 2020B1212030009).

References

Andersen, M. (2015). Unweaving the human response in daylighting design. *Building and Environment, 91*, 101-117. doi:10.1016/j.buildenv.2015.03.014

CEN/TC 169. (2018). *European Standard EN 17037: Daylight in Buildings.* Hørsholm, Denmark: European Committee for Standardization.

Chen, B., Tu, Y., Wu, S., Song, Y., Jin, Y., Webster, C., Xu, B. & Gong, P. (2022). Beyond green environments: multi-scale difference in human exposure to greenspace in China. *Environment International, 166*, 107348. doi:10.1016/j.envint.2022.107348

Choguill, C. L. (2008). Developing sustainable neighbourhoods. *Habitat International, 32*(1), 41-48. doi:10.1016/j.habitatint.2007.06.007

CIBSE. (2014). *Lighting Guide 10: Daylighting—A Guide for Designers.* London, United Kingdom: Chartered Institution of Building Services Engineers (CIBSE).

Coppel, G. & Wüstemann, H. (2017). The impact of urban green space on health in Berlin, Germany: Empirical findings and implications for urban planning. *Landscape and Urban Planning, 167*, 410-418. doi:10.1016/j.landurbplan.2017.06.015

Cox, D. T., Hudson, H. L., Shanahan, D. F., Fuller, R. A. & Gaston, K. J. (2017). The rarity of direct experiences of nature in an urban population. *Landscape and Urban Planning, 160*, 79-84. doi:10.1016/j.landurbplan.2016.12.006

Fan, P., Xu, L., Yue, W. & Chen, J. (2017). Accessibility of public urban green space in an urban periphery: The case of Shanghai. *Landscape and Urban Planning, 165*, 177-192. doi:10.1016/j.landurbplan.2016.11.007

Fisher-Gewirtzman, D. (2018). Integrating 'weighted views' to quantitative 3D visibility analysis as a predictive tool for perception of space. *Environment and Planning B: Urban Analytics and City Science, 45*(2), 345-366. doi:10.1177/0265813516676486

Hartig, T., Mitchell, R., Vries, S. D. & Frumkin, H. (2014). Nature and health. *Annual Review of Public Health, 35*, 207-228. doi:10.1146/annurev-publhealth-032013-182443

He, D., Lu, Y., Xie, B. & Helbich, M. (2022). How greenway exposure reduces body weight: A natural experiment in China. *Landscape and Urban Planning, 226*, 104502. doi:10.1016/j.landurbplan.2022.104502

He, D., Miao, J., Lu, Y. S. & Liu, Y. (2022). Urban greenery mitigates the negative effect of urban density on older adults' life satisfaction: Evidence from Shanghai, China. *Cities, 124*, 103607. doi:10.1016/j.cities.2022.103607

Helbich, M., Yao, Y., Liu, Y., Zhang, J., Liu, P. & Wang, R. (2019). Using deep learning to examine street view green and blue spaces and their associations with geriatric depression in Beijing, China. *Environment International, 126*, 107-11. doi:10.1016/j.envint.2019.02.013

HKBA. (2011). *Code of Practice for Building Works for Lifts and Escalators 2011.* Hong Kong: Building Authority.

HKEMSD. (2021). *Particulars of the Use Permit of Lifts.* Hong Kong: Electrical and Mechanical Services Department, Government of Hong Kong SAR.

HKHAD. (2021). *Database of private buildings in Hong Kong.* Hong Kong: Home Affairs Department, Government of Hong Kong SAR.

HKLandsD. (2014). *iB1000 Digital Topographic Map.* Hong Kong: Lands Department, Government of Hong Kong SAR.

HKLandsD. (2021). *3D Pedestrian Network.* Hong Kong: Lands Department, Government of Hong Kong SAR.

HKLWB. (2006). *Public Consultation on the Review of the "Design Manual: Barrier Free Access 1997".* Hong Kong: Labour and Welfare Bureau, Government of Hong Kong SAR.

HKPlanD. (2018). *Hong Kong Planning Standards and Guidelines.* Hong Kong: Planning department, Hong Kong SAR. doi:https://www.pland.gov.hk/pland_en/tech_doc/hkpsg/full/pdf/ch2.pdf

HKPlanD. (2019). *3D Photo-realistic Model.* Hong Kong: Planning Department, Government of Hong Kong SAR. Retrieved from https://www.pland.gov.hk/pland_en/info_serv/3D_models/download.htm

HKTPB. (2010). *Guidelines on submission of visual impact assessment for planning applications to the Town Planning Board.* Hong Kong: Town Planning Board. doi:https://www.info.gov.hk/tpb/en/forms/Guidelines/TPB_PG_41.pdf

Huang, B., Fery, P., Xue, L. & Wang, Y. (2008). Seeking the Pareto front for multiobjective spatial optimization problems. *International Journal of Geographical Information Science, 22*(5), 507-526. doi:10.1080/13658810701492365

Jiang, B., Chang, C.-Y. & Sullivan, W. C. (2014). A dose of nature: Tree cover, stress reduction, and gender differences. *Landscape and Urban Planning, 132*, 26-36. doi:10.1016/j.landurbplan.2014.08.005

Jiang, B., Xu, W., Ji, W., Kim, G., Pryor, M. & Sullivan, W. C. (2021). Impacts of nature and built acoustic-visual environments on human's multidimensional mood states: A cross-continent experiment. *Journal of Environmental Psychology, 77*, 101659. doi:10.1016/j.jenvp.2021.101659

Kaplan, R. (2001). The nature of the view from home: Psychological benefits. *Environment and Behavior, 33*(4), 507-542. doi:10.1177/00139160121973115

Keniger, L. E., Gaston, K. J., Irvine, K. N. & Fuller, R. A. (2013). What are the benefits of interacting with nature? *International Journal of Environmental Research and Public Health, 10*(3), 913-935. doi:10.3390/ijerph10030913

Kuo, F. E. & Sullivan, W. C. (2001). Environment and crime in the inner city: Does vegetation reduce crime? *Environment and Behavior, 33*(3), 343-367. doi:10.1177/0013916501333002

Labib, S. M., Lindley, S. & Huck, J. J. (2021). Estimating multiple greenspace exposure types and their associations with neighbourhood premature mortality: A socioecological study. *Science of The Total Environment, 789*, 147919.

doi:10.1016/j.scitotenv.2021.147919
Laovisutthichai, V., Li, M., Xue, F., Lu, W., Tam, K. & Yeh, A. G. (2021). CIM-enabled quantitative view assessment in architectural design and space planning. *38th International Symposium on Automation and Robotics in Construction (ISARC 2021).* Dubai.

Li, M., Xue, F., Wu, Y. & Yeh, A. G. (2022). A room with a view: Automated assessment of window views for high-rise high-density areas using City Information Models and transfer deep learning. *Landscape and Urban Planning, 226*, 104505. doi:10.1016/j.landurbplan.2022.104505

Li, M., Xue, F., Yeh, A. G. & Lu, W. (2021). Classification of photo-realistic 3D window views in a high-density city: The case of Hong Kong. *Proceedings of the 25th International Symposium on Advancement of Construction Management and Real Estate* (pp. 1339-1350). Wuhan: Springer, Singapore. doi:10.1007/978-981-16-3587-8_91

Lottrup, L., Stigsdotter, U. K., Meilby, H. & Claudi, A. G. (2015). The workplace window view: a determinant of office workers' work ability and job satisfaction. *Landscape Research, 40*(1), 57-75. doi:10.1080/01426397.2013.829806

Lwin, K. K. & Murayama, Y. (2011). Modelling of urban green space walkability: Eco-friendly walk score calculator. *Computers, Environment and Urban systems, 35*(5), 408-420. doi:10.1016/j.compenvurbsys.2011.05.002

Malczewski, J. & Rinner, C. (2015). *Multicriteria decision analysis in geographic information science.* New York: Springer.

Malczewski, J. (2006). GIS-based multicriteria decision analysis: a survey of the literature. *International Journal of Geographical Information Science, 20*(7), 703-726. doi:10.1080/13658810600661508

Oh, K. & Jeong, S. (2007). Assessing the spatial distribution of urban parks using GIS. *Landscape and Urban planning, 82*(1-2), 25-32. doi:10.1016/j.landurbplan.2007.01.014

Park, Y. & Guldmann, J.-M. (2020). Understanding disparities in community green accessibility under alternative green measures: A metropolitan-wide analysis of Columbus, Ohio, and Atlanta, Georgia. *Landscape and Urban Planning, 200*, 103806. doi:10.1016/j.landurbplan.2020.103806

Rahman, M. M. & Szabó, G. (2021). Multi-objective urban land use optimization using spatial data: A systematic review. *Sustainable Cities and Society, 74*, 103214. doi:10.1016/j.scs.2021.103214

Raymond, C. M., Gottwald, S., Kuoppa, J. & Kyttae, M. (2016). Integrating multiple elements of environmental justice into urban blue space planning using public participation geographic information systems. *Landscape and Urban Planning, 153*, 198-208. doi:10.1016/j.landurbplan.2016.05.005

Sun, G., Webster, C. & Zhang, X. (2021). Connecting the city: a three-dimensional pedestrian network of Hong Kong. *Environment and Planning B: Urban Analytics and City Science, 48*(1), 60-75. doi:10.1177/2399808319847204

Tang, B.-S., Wong, K. K., Tang, K. S. & Wong, S. W. (2021). Walking accessibility to neighbourhood open space in a multi-level urban environment of Hong Kong. *Environment and Planning B: Urban Analytics and City Science, 48*(5), 1340-1356. doi:10.1177/2399808320932575

Tara, A., Lawson, G. & Renata, A. (2021). Measuring magnitude of change by high-rise buildings in visual amenity conflicts in Brisbane. *Landscape and Urban Planning, 205*, 103930. doi:10.1016/j.landurbplan.2020.103930

Tobler, W. (1993). *Three presentations on geographical analysis and modeling.* Santa Barbara: National Center for Geographic Information and Analysis.

Ulrich, R. S. (1984). View through a window may influence recovery from surgery. *Science, 224*(4647), 420-421. doi:10.1126/science.6143402

USGBC. (2019). *LEED v4 for building design and construction* (4th ed.). Washington, DC, US: U.S. Green Building Council.

Wolch, J. R., Byrne, J. & Newell, J. P. (2014). Urban green space, public health, and environmental justice: The challenge of making cities 'just green enough. *Landscape and Urban Planning, 125*, 234-244. doi:10.1016/j.landurbplan.2014.01.017

Xia, C., Zhang, A. & Yeh, A. G. (2022). The varying relationships between multidimensional urban form and urban vitality in Chinese megacities: Insights from a comparative analysis. *Annals of the American Association of Geographers, 112*(1), 141-166. doi:10.1080/24694452.2021.1919502

Xue, F., Li, X., Lu, W., Webster, C. J., Chen, Z. & Lin, L. (2021a). Big data-driven pedestrian analytics: unsupervised clustering and relational query based on Tencent Street View photographs. *ISPRS International Journal of Geo-Information, 10*(8), 561. doi:10.3390/ijgi10080561

Xue, F., Wu, L. & Lu, W. (2021b). Semantic enrichment of building and city information models: A ten-year review. *Advanced Engineering Informatics, 47*, 101245. doi:10.1016/j.aei.2020.101245

Yang, L., Ao, Y., Ke, J., Lu, Y. & Liang, Y. (2021). To walk or not to walk? Examining non-linear effects of streetscape greenery on walking propensity of older adults. *Journal of Transport Geography, 94*, 103099. doi:10.1016/j.jtrangeo.2021.103099

Ye, Y., Richards, D., Lu, Y., Song, X., Zhuang, Y., Zeng, W. & Zhong, T. (2019). Measuring daily accessed street greenery: A human-scale approach for informing better urban planning practices. *Landscape and Urban Planning, 191*, 103434. doi:10.1016/j.landurbplan.2018.08.028

Zhao, J., Sun, G. & Webster, C. (2020). Walkability scoring: Why and how does a three-dimensional pedestrian network matter?. *Environment and Planning B: Urban Analytics and City Science*, 2399808320977871. doi:10.1177/2399808320977871